

The Role of Ultraviolet Imaging in Studies of Resolved and Unresolved Young Stellar Populations. M31 and M33. ☆

Luciana Bianchi^a, Yongbeom Kang^b, Paul Hodge^c, Julianne Dalcanton^c, Benjamin Williams^c

^a*Department of Physics and Astronomy, The Johns Hopkins University, 3400 N.Charles Street, Baltimore, MD 21218, USA*

^b*Dept. of Astronomy and Space Science, Chungnam University, 220 Gun-dong, Daejeon 3-5-764, South Korea, and visitor at The Johns Hopkins University, Dept. of Physics and Astronomy, 3400 N.Charles Street, Baltimore, MD21218, USA; currently at Korea Astronomy and Space Science Institute, 776 Daedeokdae-ro, Yuseong-gu, Daejeon, 305-348 Republic of Korea*

^c*Department of Astronomy, University of Washington, Box 351580, Seattle, WA 98195, USA*

Abstract

We discuss the relevance of UV data in the detection and characterization of hot massive stars and young stellar populations in galaxies. We show results from recent extensive surveys in M31 and M33 with *Hubble Space Telescope* (HST) multi-wavelength data including UV filters, which imaged several regions at a linear resolution (projected) of less than half a pc in these galaxies, and from GALEX far-UV and near-UV wide-field, low-resolution imaging of the entire galaxies. Both datasets allow us to study the hierarchical structure of star formation: the youngest stellar groups are the most compact, and are often arranged within broader, sparser structures. The derived recent star-formation rates are rather similar for the two galaxies, when scaled for the respective areas. We show how uncertainties in metallic-

☆Based on data from the Hubble Space Telescope and from GALEX

Email addresses: bianchi@pha.jhu.edu (Luciana Bianchi), ybkang@pha.jhu.edu (Yongbeom Kang), hodge@astro.washington.edu (Paul Hodge), jd@astro.washington.edu (Julianne Dalcanton), ben@astro.washington.edu (Benjamin Williams)

URL: <http://dolomiti.pha.jhu.edu> (Luciana Bianchi)

ity and type of selective extinction for the internal reddening may affect the results, and how an appropriate complement of UV filters could reduce such uncertainties, and significantly alleviate some parameter degeneracies.

Keywords: Ultraviolet: imaging, Stars: massive stars, Stars: stellar parameters, Galaxies: star formation, Galaxies: M31, M33 Ultraviolet: galaxies

1. Introduction

Much interest and major observational and theoretical efforts in current astrophysics research are devoted to understanding star formation. How and when did the current baryon/stellar mass form throughout the history of the universe? What are the triggering and regulating factors?

Hot massive stars are fundamental players in galaxy evolution, because of their input to the chemical and dynamical evolution of the interstellar medium (ISM). Through supernova (SN) explosions, they drive stellar feedback on galactic scales. They also produce dust, in their late stages, and modify dust grain properties in their early evolutionary stages, when they emit powerful Ultraviolet (UV) radiation. Because they evolve on very fast time-scales, they are a powerful tool to trace, and to precisely age-date, star-formation episodes. Very luminous, they dominate the light of starburst galaxies and can be detected at large distances. Therefore, understanding the formation, evolution, and mass distribution of massive stars is critical for interpreting the integrated light of distant galaxies, for correctly modeling the chemical evolution of galaxies, and ultimately to unravel the history of star formation in the universe, in terms of stellar mass formed and energy balance.

The local universe, and the Local Group of galaxies (LG) in particular, offer an ideal laboratory for resolved stellar population studies, probing a wide variety in galaxy type, mass, gas content, metallicity, environment. Results from such studies can be used to calibrate global star-formation indicators, and population synthesis models for interpreting the light of more distant galaxies.

Rest-frame Ultraviolet data are critical both to unambiguously identify massive stars and to measure their physical parameters. Similarly, they are critical to characterize unresolved young stellar populations, and ISM dust. In this paper we will address one aspect of the role of UV data in the char-

acterization of star-forming sites through their hot massive star content. We will restrict our focus to broad-band imaging and photometry of both resolved and unresolved young stellar populations. Such imaging can be afforded for large samples of star-forming sites and entire galaxies; abundant results and rich databases have been recently provided by several instruments. Among them, the Galaxy Evolution Explorer (GALEX) and the Hubble Space Telescope (HST) represent the two most conspicuous sources, from the point of view of our present focus, and two extreme examples as for the trade-off between field of view and spatial resolution. We will limit our discussion to the two nearest spiral galaxies, M31 and M33, where recent UV surveys have been performed or are ongoing. Some discussion on UV imaging of Local Group dwarfs can be found e.g., in Bianchi et al. (2012a, 2011) and references therein, and Wyder et al. (2009).

Ultraviolet wavelengths provide other essential diagnostics, through spectroscopy, in particular for estimating hot stars parameters (e.g. Bianchi & Garcia, 2013; Bianchi 2012 and references therein). Currently, however, UV spectroscopy can be afforded for very small samples, given the lack of multi-slit capabilities (if we except GALEX grisms, and grisms in some HST imagers, that do not provide sufficient resolution for detailed line analysis). It is also limited to the brightest massive stars in the Local Group, a medium-resolution UV spectrum requiring a few orbits -long observations with HST for example, at the distance of M31 and M33. Such scant spectroscopic samples are nonetheless of fundamental importance to validate and calibrate the photometric derivation of global parameters, available for large samples, often for entire star-forming sites.

The paper is arranged as follows. In Section 2 we illustrate the role of UV filters in deriving stellar parameters and extinction by interstellar dust, for hot massive stars in particular, using examples from existing HST imagers, and sample results for M31 and M33. In Section 3 we compare results from wide-field GALEX data of the same galaxies. In Appendix A we provide stellar model magnitudes in some representative band-passes discussed in this paper, which may be useful to others for analysis of the abundant GALEX and HST archival data and for planning dedicated UV observations.

2. HST surveys: the detailed view of star-forming sites

Ever since HST was launched, several observing programs every year have been dedicated to the study of stellar populations in nearby galaxies, and

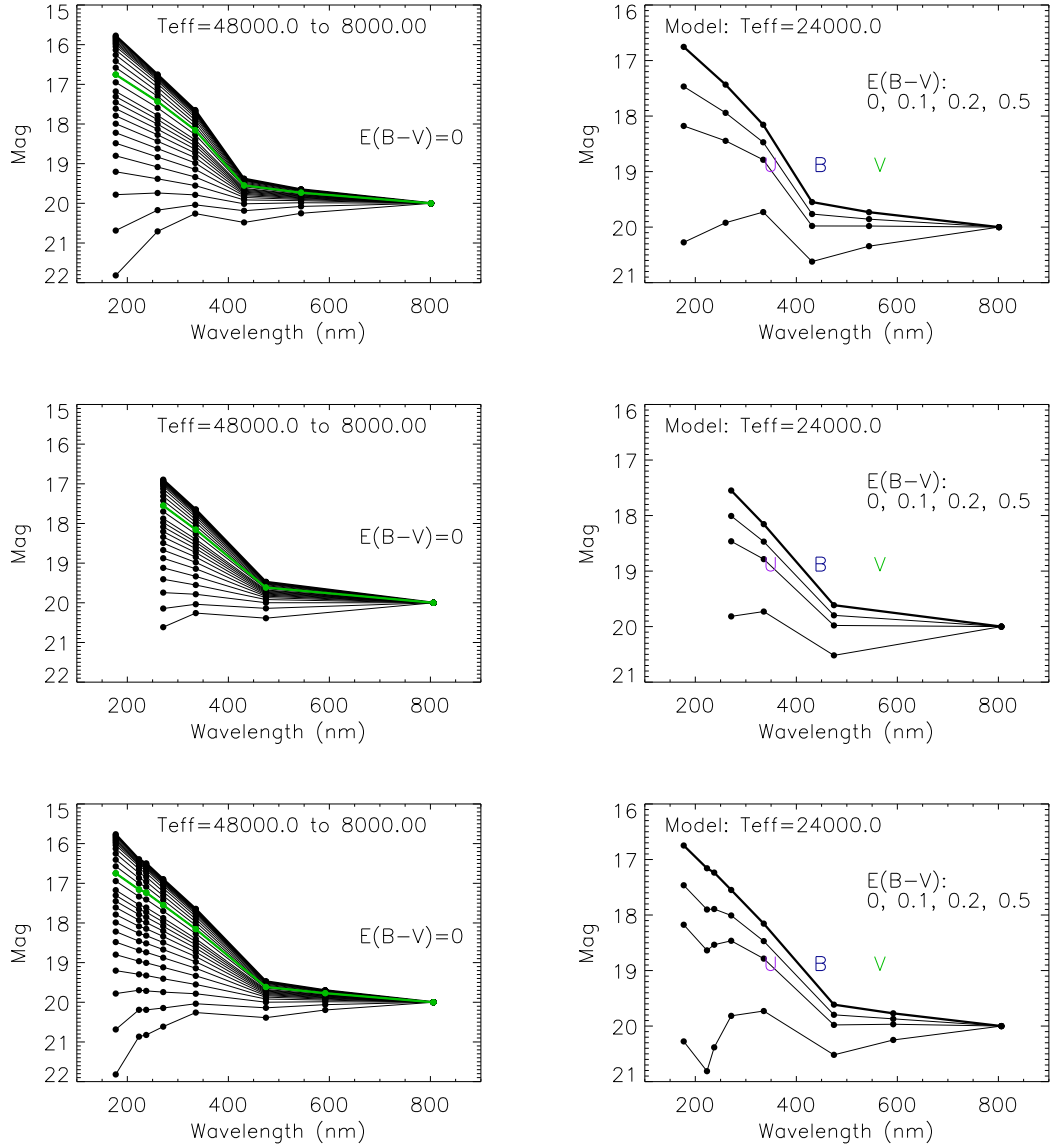


Figure 1: The importance of UV filters to discern interstellar extinction effects from physical parameters (T_{eff}) for hot stars. The left plots show broad-band model magnitudes (SEDs) for a range of T_{eff} , and the right plots the SEDs for one value of T_{eff} (24kK, shown in green/grey in the left-side plots), with increasing reddening amounts. Colors of hot stars become progressively saturated in optical bands, and the degeneracy between reddening and T_{eff} more severe. Model magnitudes are shown for HST filters: top row for Bianchi's treasury survey TrImS, which included a FUV filter, second row for PHAT filters. The third row shows a rich complement of several filters (HST's WFC3's UVIS-F218W and UVIS-F225W, in addition to WFC2 F170W and the 4 optical PHAT filters). Such redundancy could not be afforded so far, due to the demanding exposures, but would be decisive in removing the degeneracy between T_{eff} and the amount, and type, of reddening. Model magnitudes are plotted at the band-pass λ_{eff} ; λ_{eff} of classical U, B, V filters are also marked (right panels).

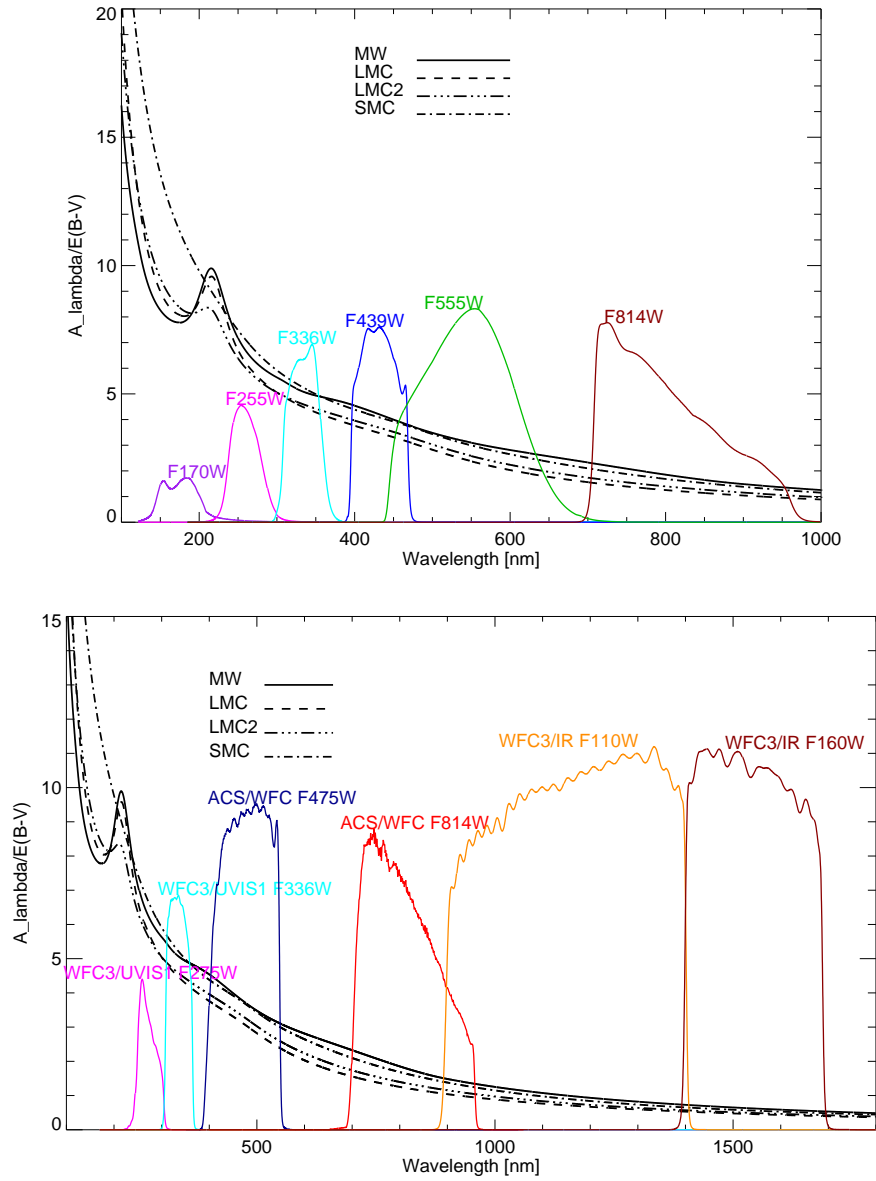


Figure 2: Transmission curves of HST filters used in two recent surveys: TrImS (top, star-forming regions in M31, M33, and dwarfs; Bianchi et al. 2012a,b) and PHAT (bottom, M31). The filters are from HST cameras widely used for stellar populations studies: Wide-Field Planetary Camera-2 (WFPC2), Advanced Camera for Surveys (ACS), Wide-Field Camera 3 (WFC3). Examples of selective extinction curves for known sight-lines (see text, also Bianchi 2011 for reddening coefficients) illustrate the sensitivity of UV data to interstellar extinction

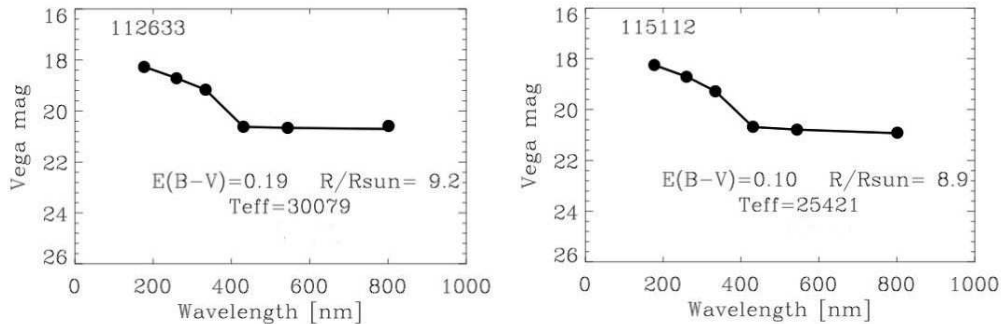


Figure 3: Examples of SED fitting: two hot stars in M31 OB 99 (Bianchi et al.2012b). Dots are observed photometry (errors are smaller than the dot size); best-fit model magnitudes are connected by lines. Reddening and T_{eff} are derived concurrently.

especially within the LG, too many to even attempt a representative list or summary of highlights. The resolution of HST cameras of $\leq 0.1''$ /pxl translates into linear scales in the Local Group from ≤ 0.2 pc in the nearby Phoenix dwarf to ≤ 0.4 pc at the distance of M31 and M33. One relevant outcome of HST studies is that most sources in ground-based catalogs of LG galaxies turned out to be multiple stars. Very high resolution is necessary for a conclusive census, even for the most luminous, hottest stars, although they are extremely rare (the stellar mass function being skewed towards low masses), because they are usually formed in the dense cores of star-forming clouds, and therefore are found in compact groups. The advantage of HST's $\gtrsim 10\times$ better resolution with respect to traditional ground-based telescopes, for LG studies, cannot be overemphasized. On one hand, stellar counts underpin many science results (Initial Stellar Mass Function: IMF, mass estimate of resolved clusters and O-B associations, clustering properties); what's more, magnitudes and colours of a source composed of two or few unresolved stars are misleading for deriving stellar parameters. Even considering surveys with rather bright completeness limits, such as the ground-based *Local Group Galaxies Survey* (LGGS, Massey et al. 2006) and Bianchi's HST program 10079 *Hubble Treasury Imaging of Star Forming Regions in the Local Group* (TrImS), the fraction of ground-based sources that turned out to be multiple sources in HST imaging range between 50% and 80% (depending on environment) within a sample of six dwarfs (Bianchi et al. 2012a). The brightness of composite sources is by consequence overestimated, by up to significant

extents (see Fig. 3 of Bianchi et al. 2012a), and their colors meaningless for the derivation of stellar parameters. Yet, such ground-based catalogs are up to now the only available datasets with significant coverage for extended galaxies, and for this reason are widely used for studies of stellar populations or estimates of internal extinction (e.g. Bastian et al. 2009, Kang et al 2009), the biases being unavoidable.

For the study of hot stars, HST provides another critical advantage with respect to ground-based data, in addition to the spatial resolution: its access to space UV wavelengths. Optical colors are saturated at the high temperatures of O- and early-B type stars, becoming insensitive to discern the hottest O types: yet the difference in luminosity, ionizing photons, and age-dating diagnostics between an early- and late-O star is huge and such degeneracy limits the results from young stellar populations studies. For example, there is a mass difference $\gg 2$ between a $T_{\text{eff}}=30,000\text{K}$ and a $T_{\text{eff}}=50,000\text{K}$ star, but their optical colors are undistinguishable with typical photometric errors, while a UV–optical color may differ by over half magnitude (e.g. Bianchi et al. 2012a, see also Table A.1 in appendix). In addition to the saturation of the intrinsic colors in optical filters, the degeneracy between T_{eff} and reddening is more severe for hot stars. As these emit the bulk of their energy in UV, and UV fluxes are also more affected by reddening, the combination of UV and optical colors largely alleviates such degeneracies, and provides more sensitive diagnostics.

Figures 1 and 2 illustrate the role of UV filters discussed above, through the example of stellar model colors computed in filters of HST cameras most used in studies of stellar populations. Our sample plots show a few filters each, for clarity, and also because for practical reasons each program is confined to a limited choice: we include filters from two recent surveys discussed below (TrImS and PHAT, first and second row panels). The figures (top and bottom panels) show that ideally two UV filters shortwards of the U-band can remove the degeneracy between T_{eff} and reddening, and increase sensitivity to identify the hottest stars. This can rarely be afforded due to the demanding exposure times in such filters. The majority of the HST observing programs are focused on optical and IR bands, exploiting HST’s high resolution for studying old stellar populations, to unravel the past star-formation history (SFH) of galaxies, a complementary aspect to the topic discussed in this work.

2.1. Recent HST surveys of M31 and M33

The TrImS program imaged 67 star-forming regions in M31, M33 and 6 dwarf galaxies in the LG (Bianchi et al. 2011, 2012a, b, 2013b, Hodge et al. 2010, 2011), with 6 filters, far-UV ($\sim 170\text{nm}$), near-UV ($\sim 255\text{nm}$), and \approx U, B, V and I bands, for a total of 882 HST images. The band-passes are shown in Figure 2. This program provided resolved maps of hot stars and extinction in many (in some cases all) of the most conspicuous star-forming (SF) sites in these galaxies, and allowed us to examine their characteristics and the variation of hot massive stars content among them. The 22 regions studied in M31, for example, range from the richest associations OB54 and OB78, having over 600 hot stars in a $\sim 3'$ -wide HST field (OB 78 extends over two fields, with a total of >1200 hot stars), as well as the highest reddenings among the sample (average $E_{B-V} \sim 0.45\text{mag}$), to the outermost regions OB184 and OB157 at almost 22kpc and 21kpc from the galaxy center (S and N respectively), with an average $E_{B-V} \lesssim 0.12\text{mag}$, i.e. almost entirely foreground, and 138/ 48 hot stars respectively.

Most HST programs have been limited to high-priority fields, given the small field-of-views, which typically encompass the size of an O-B association in LG galaxies. The large multi-cycle Panchromatic Hubble Andromeda Treasury [program] (PHAT) (Dalcanton et al. 2012) is for the first time mapping a contiguous large portion (about one third) of M31, at HST resolution and quality, with a near-UV (F275W), a U-band (F336W), a blue (F475W), an \sim I (F814W), and two IR filters. The mapping proceeds by progressively tiling “bricks” (3×6 contiguous HST fields each). At the end of the program, after over 800 orbits spent, we expect an unprecedented catalog of the order of a hundred million M31 stars.

From both programs we have analyzed the broad-band spectral-energy distribution (SED) of each stellar source with model magnitudes (such as those shown in Figure 1), and derived E_{B-V} and T_{eff} , as well as radius and luminosity (since the distance to the galaxy is known). Examples can be seen in Figure 3. From the ensemble of the results, we obtain maps of the measured stars with their physical parameters, as shown in Figure 4 for PHAT’s Brick 15, which includes a major portion of a Northern spiral arm and the rich association OB 54. Similar maps are shown by Bianchi et al. (2012b) for all the 22 conspicuous SF regions in M31 from TrImS, by Bianchi et al. (2013a) for five PHAT bricks with complete filter coverage, and by Bianchi et al. (2013b) for 36 star-forming regions in M33.

2.2. Spatial Clustering of the Young Populations

The maps presented in the previous session show, with the detail of individual-star measurements, the hierarchical nature of the star-formation process, postulated by current theories and by observations of the Milky Way and the Magellanic Clouds (e.g., Elmegreen 2008). The hottest stars tend to cluster in compact groups, which in turn are arranged often within larger complexes; longer-lived stars (such as B-types) abound in the same areas but are distributed in sparser structures, consistent with the dynamical evolution of unbound O-B associations.

With multi-wavelength photometry we infer individual stellar parameters, and can reliably identify hot stars thanks to the UV colors, therefore we can also quantify their spatial structuring. Bianchi et al. (2012b, 2013a) have applied clustering (near-neighbor) algorithms to define O-B associations, on a range of spatial scales. Stars are deemed associated if they are closer to each other than an adopted “link-distance”; by varying the link distance from $2''$ to $6''$ for example, we define from compact to sparse associations. We construct in this way samples of O-B associations throughout the imaged areas. An example of associations defined on two different scales is shown in the bottom panel of Figure 5

By extrapolating the hot-star counts with an assumed IMF, we can estimate the stellar mass in each defined association. Figure 6 shows the cumulative distribution of masses for M31 associations, on the left from TrImS (targeting only conspicuous SF sites), and on the right from five PHAT bricks which include a mixture of SF sites as well as sparse areas in between spiral arms. While the coverage of field regions is not yet sufficient to discern an environmental dependence, both samples clearly show that a logarithmic slope with exponent ~ 2 , as found in most stellar-cluster samples, also represents well the mass spectrum of the young O-B associations. It also shows that, in more detail, the slope depends on the spatial scale on which the structuring has been defined. This effects had been noted first by Hodge (1986) comparing galaxies at different distances. Biases that may affect mass estimates of O-B associations include the fraction of unresolved binaries (causing an underestimate of star counts, hence of the total mass), uncertainties in T_{eff} and therefore in the hot-star selection, due to the metallicity and type of selective extinction being often undetermined, stochasticity (especially severe for small associations), etc. See Bianchi et al. (2012b, 2013a) for more discussion.

3. The global view: GALEX wide-field UV imaging

GALEX (Martin et al. 2005, Morrissey et al. 2007, Bianchi 2009, 2011) has provided extensive imaging surveys at Ultraviolet wavelengths. Several papers in this publication describe the GALEX data and available databases (e.g., Bianchi et al. 2013; Conti et al. 2013, Simons et al. 2013). GALEX observed in two Ultraviolet bands, FUV ($\lambda_{eff} \sim 1528\text{\AA}$, 1344-1786 \AA) and NUV ($\lambda_{eff} \sim 2310\text{\AA}$, 1771-2831 \AA), with a wide field of view ($\approx 1.2^\circ$ diameter) at a FUV/NUV spatial resolution of $\approx 4.2/5.3''$ (Morrissey et al. 2007); the images are sampled with virtual pixels of $1.5''$ size.

The very wide field of view provided unprecedented overviews of entire large galaxies in the UV, the FUV sensitivity to hot stars (and the low sky background) revealed the presence of hot stars even in sites with extremely low star-formation rates, where star formation was never detected before, and was believed to not be possible based on established relations between gas surface density and star-formation (e.g., Bianchi 2011 and references therein, Marino et al. 2011, Thilker et al. 2007). In particular, a dedicated survey (Nearby Galaxies Survey, NGS, Bianchi et al. 2003, Gil de Paz et al. 2007), imaged hundreds of large nearby galaxies.

Early GALEX imaging of M31 and M33 was first shown by Thilker et al. (2005). Kang et al. (2009, 2013) used GALEX images to define star-forming (SF) sites from FUV-flux contours in M31 and M33. Ages and masses of the SF regions were derived from their integrated FUV and NUV fluxes, compared with population synthesis models, assuming approximately co-eval populations in the defined regions, which trace localized episodes.

Figure 5 shows two regions in M31, in GALEX FUV/NUV colors (left panels, resolution of $\sim 17\text{pc}$ in M31), and the resolved view (with individual stars color-coded by their derived T_{eff}) from HST. As noted above and elsewhere (e.g. Bianchi 2011 and references therein), FUV imaging provides a clear snapshot of the hot-star content across galaxies, unambiguously revealing their presence, while at optical wavelengths several generations and types of stars contribute to the overall light, and the young populations are harder to discern. We already noted the sensitivity afforded by UV colors for age-dating integrated populations up to a few hundred Myr (e.g., see also Figure 7 of Bianchi 2009, and Bianchi 2011).

In the top panels of Figure 5 one can appreciate a remarkable correspondence between the bluest (FUV-bright) features in the GALEX image and hot-star groups in the HST maps. But there is also a clear correspondence

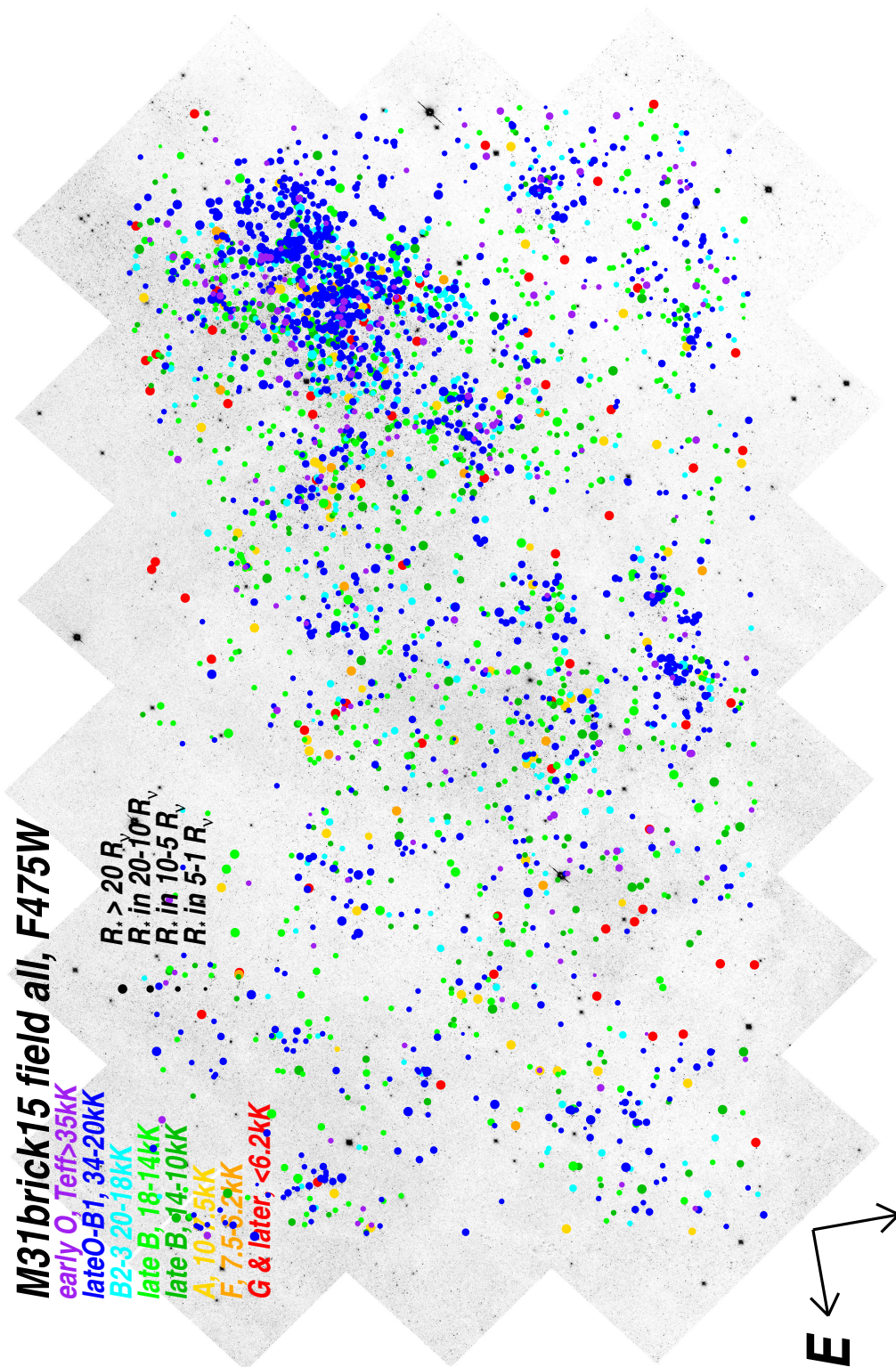


Figure 4: Map of stars color-coded by T_{eff} for PHAT's Brick 15 in M31. The size of the dots indicates the derived stellar radius. Only the brightest sources with good photometry in all filters including F275W are plotted, a selection which favours the hottest sources. When we remove this restriction, a more diffuse, much more numerous population of cooler stars is seen, reflecting the galactic global structure, but with no compact groups (see Fig. 5).

between some structures brighter in NUV (yellowish in the GALEX panels) and overdensities of intermediate-temperature stars (green dots) in the PHAT maps, in spite of some “striping” caused by deeper exposures where HST fields overlap, enhancing the density of cooler (fainter) stars in the PHAT maps. Second-row panels show a dimmer, sparser region, demonstrating the sensitivity of GALEX for detecting emission even from single hot stars. In spite of the low resolution, star-forming regions appear always “clumpy” in GALEX FUV imaging, because of the noted spatial clustering of the young hot stars, whereas these galaxies have a very smooth appearance in optical images due to the diffuse, older populations.

In Figure 7 we show a GALEX FUV/NUV image of M33 (left), and SF regions defined from contours of FUV flux (from Kang et al. 2013), with a procedure similar to that developed by Kang et al. (2009) for M31. The right panel, and the zoomed-out portion at the bottom, illustrate again the hierarchical structure of star formation, here captured by contours of FUV flux level defined at varying thresholds (see Kang et al. 2009 for extensive discussion). A portion of the regions in the bottom panels is further enlarged in Figure 8, where the FUV-defined contours are shown again, along with individual stars measured from TrImS (Bianchi et al. 2013b).

The masses of the SF regions, estimated from GALEX integrated measurements of SF sites, can be added in separate age ranges, to obtain an average star-formation rate (SFR) over these epochs (Kang et al. 2009, 2013). Figure 8 shows such SFR per unit area (assuming disks of 26 and 8kpc for M31 and M33 respectively, corresponding to the extent of the GALEX measurements), for both galaxies. Such estimates have been derived assuming different metallicities, and different cases of reddening type: Figure 9 shows how the uncertainty in metallicity propagates in the derived SFR. Other examples of uncertainties from assumed reddening curves are shown by Bianchi et al. (2011a). Such uncertainties are to date still conspicuous; they could be greatly reduced with extensive spectroscopic surveys, and by imaging with more extensive UV filter coverage.

4. Conclusions and Summary

UV–optical studies of star-forming sites in the Local Group provide a census of the hot massive stars (once they emerge from the dust cocoon of their parent giant molecular cloud), and enable the derivation of their physical parameters and reddening. A characterization of young stellar populations

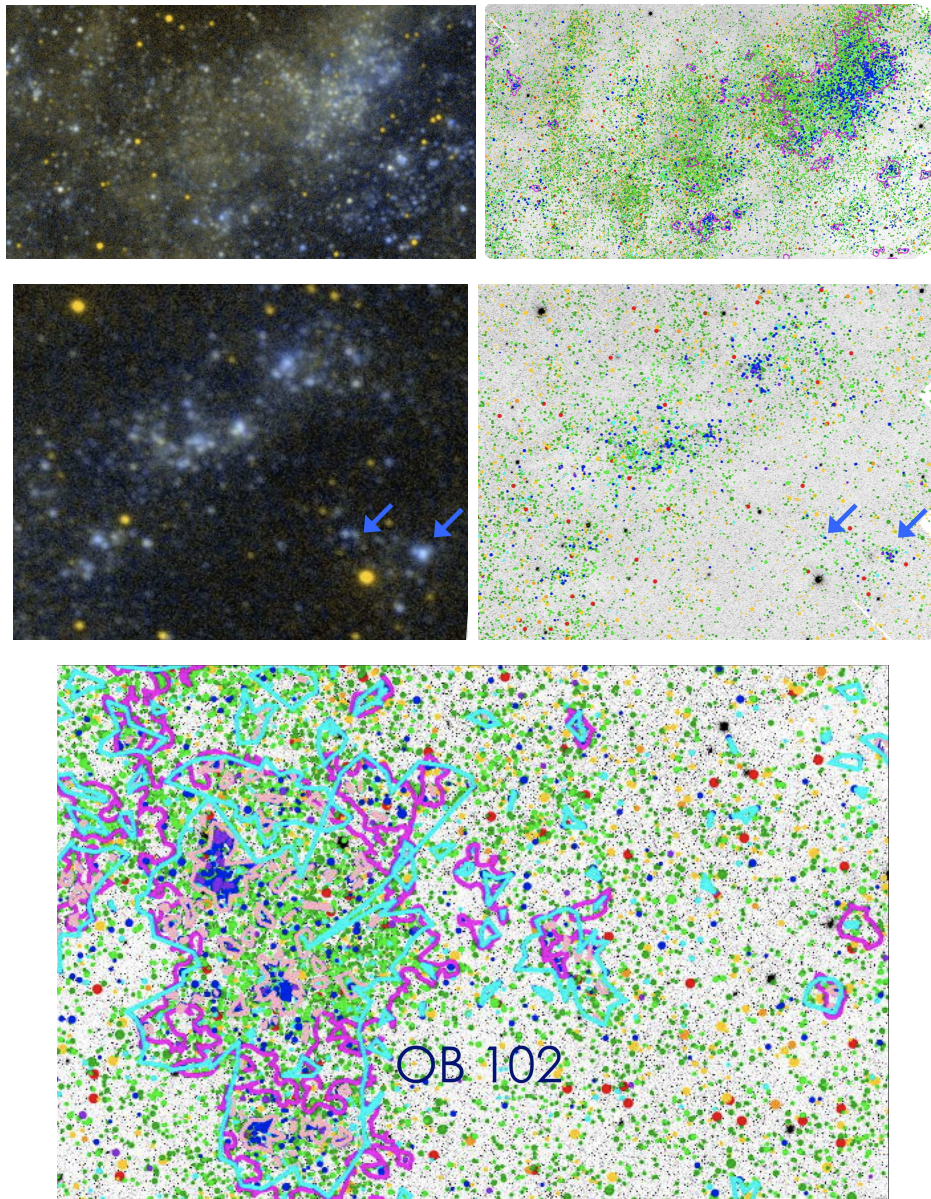


Figure 5: Star forming regions in M31, seen with GALEX (left: FUV in blue, NUV in yellow) and HST (right, from the PHAT program, with stars as dots color-coded by T_{eff}). Portions of PHAT Brick 15 (top) and Brick 21 (second row) are shown. Note the sensitivity afforded by GALEX for detecting presence of hot stars, also benefiting from the high FUV contrast over cooler stars and sky background. The bottom panel shows O-B associations contours defined from the hot stars individually measured with HST (pink and cyan, with link-distances of 3 and 5'' respectively) and the GALEX FUV-defined contours from Kang et al. 2009 (magenta).

in a variety of environmental conditions is emerging. The aspects addressed here, within the specific scope of this work, are complemented by studies of the stellar cluster systems (e.g., Johnson et al. 2012, Kang et al. 2012, Hodge et al. 2010, to cite only some recent examples in M31: for the young clusters in particular UV data are critical for age-dating - see e.g., Bianchi 2011). Combining these efforts with studies of HII regions (e.g., Hodge et al. 2011), IR dust emission, and gas, we can build a complete picture and gain a better understanding of galaxy evolution.

The rest-frame UV light of luminous star-forming galaxies such as M31, and of UV-bright star-burst galaxies, dominates the sources that *the James Webb Space Telescope* (JWST) will see out to red-shift ~ 8 , and optical surveys see in the range $2 \lesssim z \lesssim 4$. Progress in understanding the UV properties of the local universe is the stepping stone underpinning the interpretation of large samples of distant luminous galaxies from ongoing and future optical and IR surveys such as *the Panoramic Survey Telescope & Rapid Response System* (Pan-STARRS), the *Sloan Digital Sky Survey* (SDSS), and in the future *The Large Synoptic Survey Telescope* (LSST), and JWST. We have highlighted in this work the role of multi-wavelength data, and UV imaging in particular, towards this goal. We have shown results from recent surveys in M31 and M33, and stressed how the derived physical parameters of the young stellar populations strongly depend on our knowledge of dust properties and their relation to star-formation. A complement of filters such as those that will be available in *The Ultraviolet Imaging Telescope* (UVIT, to be launched soon on Indian ASTROSAT) including grisms (Kumar et al. 2012), and *The World Space Observatory* (WSO) with dedicated UV spectroscopic capabilities (Shustov et al. 2011, Gomez de Castro et al. 2011) will enable decisive advances in this field.

Acknowledgements: We thank the referees for a careful checking of the original version. This work was partly supported by NASA grants HST-GO-10079 and HST-GO-12055.02-A from the Space Telescope Science Institute, which is operated by the Association of Universities for Research in Astronomy, Inc.

Bastian, N. Ercolano, B., & Gieles, M. Hierarchical star formation in M33: properties of the star-forming regions. *Astrophysics & Space Science*, 324, 293-297. 2009

- Bianchi, L. GALEX and star formation. *Astrophysics & Space Science*, 335, 51-60, DOI: 10.1007/s10509-011-0612-2. 2011
- Bianchi, L. The Ultraviolet sky surveys: filling the gap in our view of the Universe. *Astrophysics & Space Science*, 320, 11-19. 2009
- Bianchi, L. New Advances in the Field of Planetary Nebulae from Ultraviolet Observations. in “Planetary Nebulae: An Eye to the Future”, editors A. Manchado, L. Stanghellini and D. Schnoberner, Cambridge University Press, Proceedings IAU Symposium N. 283, pp. 45-52
- Bianchi, L. & Garcia, M., The Effective Temperatures of O-type Stars from UV Spectroscopy. This publication. 2013
- Bianchi, L., Efremova, B., Hodge, P., et al. A Treasury Study of Star-forming Regions in the Local Group. I. HST Photometry of Young Populations in Six Dwarf Galaxies. *AJ*, 143, 74-98 2012a (TrImS)
- Bianchi, L., Efremova, B., Hodge, P., et al. A Hubble Space Telescope Treasury Study of Star-forming Regions in the Local Group. II. Young Stellar Populations in M31. *AJ*, 144, 142-166 2012b (TrImS)
- Bianchi, L., Kang, Y.-B., Hodge, P., et al. The Panchromatic Hubble Andromeda Survey. A first Look at the Content and Spatial Structuring of Hot Massive Stars, and the Recent Star Formation. In preparation. 2013a
- Bianchi, L., Kang, Y.-B., Hodge, P., et al. A Hubble Space Telescope Treasury Study of Star-forming Regions in the Local Group (TrImS). III. Young Stellar Populations in M33. In preparation. 2013b
- Bianchi, L., Kang, Y. B., Efremova, B., et al. Young Stellar Populations in the Local Group: an HST and GALEX comprehensive study. *Astrophysics & Space Science*, 335, 249-255. DOI: 10.1007/s10509-011-0697-7 .2011.
- Bianchi, L., Madore, B., Thilker, D., et al. The GALEX Nearby Galaxies Survey (NGS). in “The Local Group as an Astrophysical Laboratory”, STScI electronic publication Series (Baltimore), M. Livio & T. Brown eds., pp.10-15. 2003
- Conti, A., Bianchi, L., Chopra, N., et al. A database of UV Variables from the GALEX survey. This publication, DOI: <http://dx.doi.org/10.1016/j.asr.2013.07.022>. 2013

- Dalcanton, J., Williams, B., Lang, D., et al. The Panchromatic Hubble Andromeda Treasury. *ApJS*, 200, 18-54. 2012
- Elmegreen, B. Formation and Evolution of Young Massive Clusters. *ASP Conf.Ser.*, 388, 249-261 2008
- Gil de Paz, A., Boissier, S., Madore, B., et al. The GALEX Ultraviolet Atlas of Nearby Galaxies. *ApJS*, 173, 185-255. 2007
- Gomez de Castro, A.I., Maíz-Apellániz, J., Rodríguez, P., et al. The imaging and slitless spectroscopy instrument for surveys (ISSIS) for the world space observatory-ultraviolet (WSO-UV). *ApSS*, 355, 283-289 2011
- Hodge, P., Krienke, G.K. & Bianchi, L. A Morphological Study of UV-Bright Stars and Emission Nebulae in a Selection of Star Formation Regions in M31 *PASP*, 123, 649-658. 2011.
- Hodge, P., Krienke, O.K., Bianchi, L., et al. A Photometric Catalog of 77 Newly Recognized Star Clusters in M31. *PASP*, 122, 745-752. 2010
- Hodge, P. W. Systems of stellar associations in galaxies. *IAU Symp.* 116, 369-378. 1986
- Johnson, L.C., Seth, A. C.; Dalcanton, J., et al. PHAT Stellar Cluster Survey I. Year I Catalog and Integrated Photometry. *ApJ*, 752, 95-116. 2012
- Kang, Y.-B., Bianchi, L., & Rey, S.-C. An Ultraviolet Study of Star-Forming Regions in M31. *ApJ*, 703, 614–627. 2009
- Kang, Y.-B., Rey, S.-C., Bianchi, L., et al., A Comprehensive GALEX Ultraviolet catalog of Star Clusters in M31 and a Study of the Young Clusters. *ApJS*, 199, 37-61. 2012
- Kang, Y.-B., Bianchi, L., et al. In preparation. 2013
- Kumar, A., Ghosh, S. K., Kamath, P. U., et al, Tests and calibration on ultraviolet imaging telescope (UVIT). in “Space Telescopes and Instrumentation 2012: Ultraviolet to Gamma Ray. Proceedings of the SPIE”, Volume 8443, 4-13, id. 84431N-84431N-12. 2012

- Marino, A., Bianchi, L., Rampazzo, R., et al. Signatures of recent star formation in nearby S0 galaxies. *Astrophysics and Space Science*, 2011, 335, 243-248. 2011
- Massey, P., Olsen, K. A. G., Hodge, P. W., Strong, S. B., Jacoby, G. H., Schlingman, W., & Smith, R. C.A Survey of Local Group Galaxies Currently Forming Stars. I. UBVRI Photometry of Stars in M31 and M33. *AJ*, 131, 2478-2496. (LGGS) 2006
- Martin, D. C., Fanson, J., Schiminovich, D., et al. The Galaxy Evolution Explorer: A Space Ultraviolet Survey Mission. *ApJl*, 619, L1-6 2005
- Morrissey, P., Conrow, T., Barlow, T., et al. The Calibration and Data Products of the Galaxy Evolution Explorer. *ApJS*, 173, 682-697. 2007
- Shustov, B., Sachkov, M., Gomez de Castro, A.-I., et al. World space observatory-ultraviolet among UV missions of the coming years. *ApSS*, 335, 273-282. 2011
- Simons, R. Thilker, D., & Bianchi, L., et al. The Ultraviolet View of the Magellanic Clouds from GALEX: A First Look at the LMC Source Catalog. This publication (DOI: <http://dx.doi.org/10.1016/j.asr.2013.07.016>). 2013
- Thilker, D., Hoopes, C., Bianchi, L., et al. Panoramic GALEX Far- and Near-Ultraviolet Imaging of M31 and M33. *ApJ*, 619, L67-70. 2005.
- Thilker, D., Bianchi, L., Meurer, G., et al. A Search for Extended Ultraviolet Disk galaxies in the Local Universe. *ApJS*, 173, 538-571. 2007
- Wyder, T., Martin, C., Barlow, T., et al. The Star Formation Law at Low Surface Density. *ApJ*, 696, 1834-1853. 2009

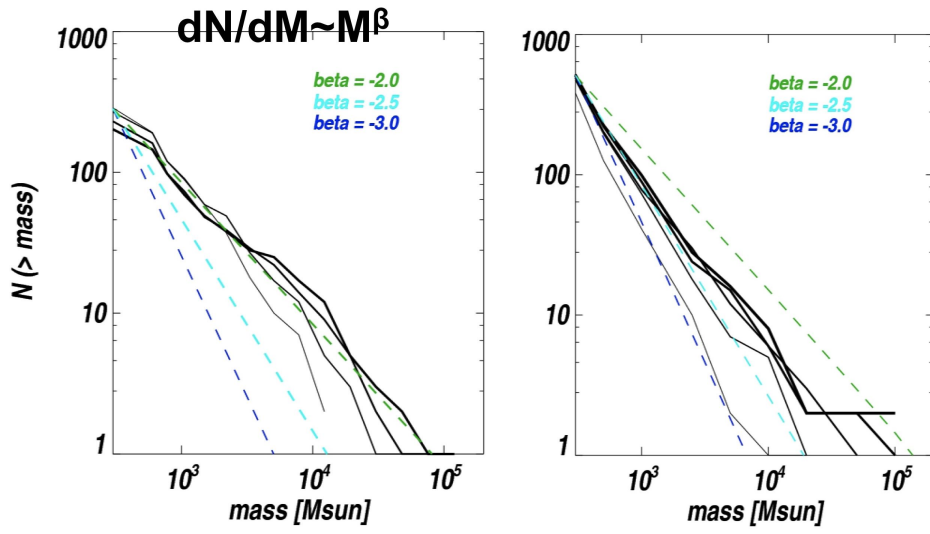


Figure 6: Cumulative distribution of masses of O-B associations in M31, estimated from counts of hot stars, and defined for different link distances (3 to 6'' , thin to thick lines); results from Bianchi et al. (2012b) HST program which targeted only conspicuous regions are shown on the left, and results from the early PHAT observations (Bianchi et al. 2013a) which samples also sparse environments are shown on the right.

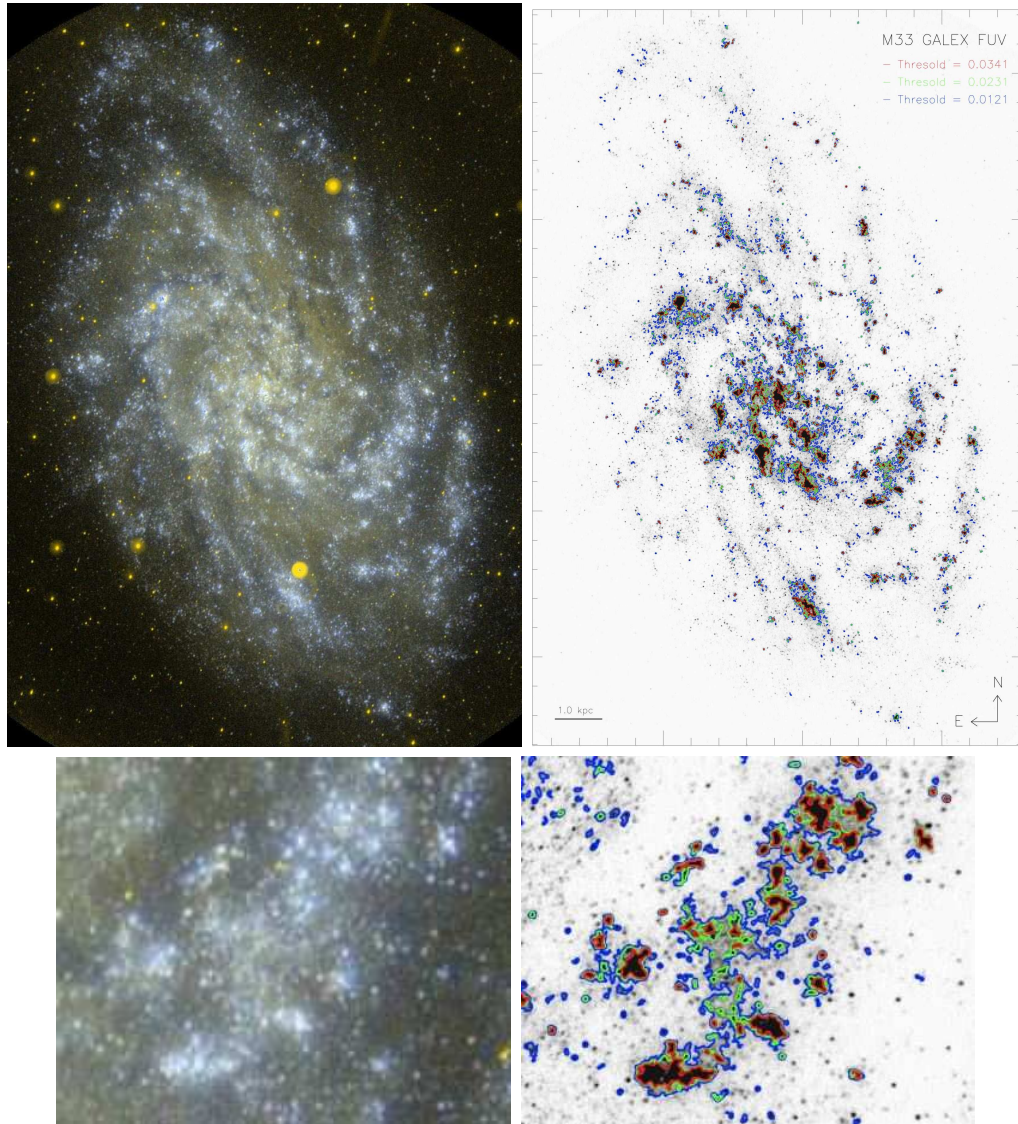


Figure 7: M33 as seen by GALEX (left: FUV in blue, NUV in yellow) and contours of SF regions defined from the FUV GALEX imaging (right, adapted from Kang et al. 2013). A portion from the SW inner spiral arm is enlarged in the lower panels: it illustrates the clustering of hot stars on hierarchical structures, here captured by different flux-threshold contours, and shown in the previous figures from individual-star photometry.

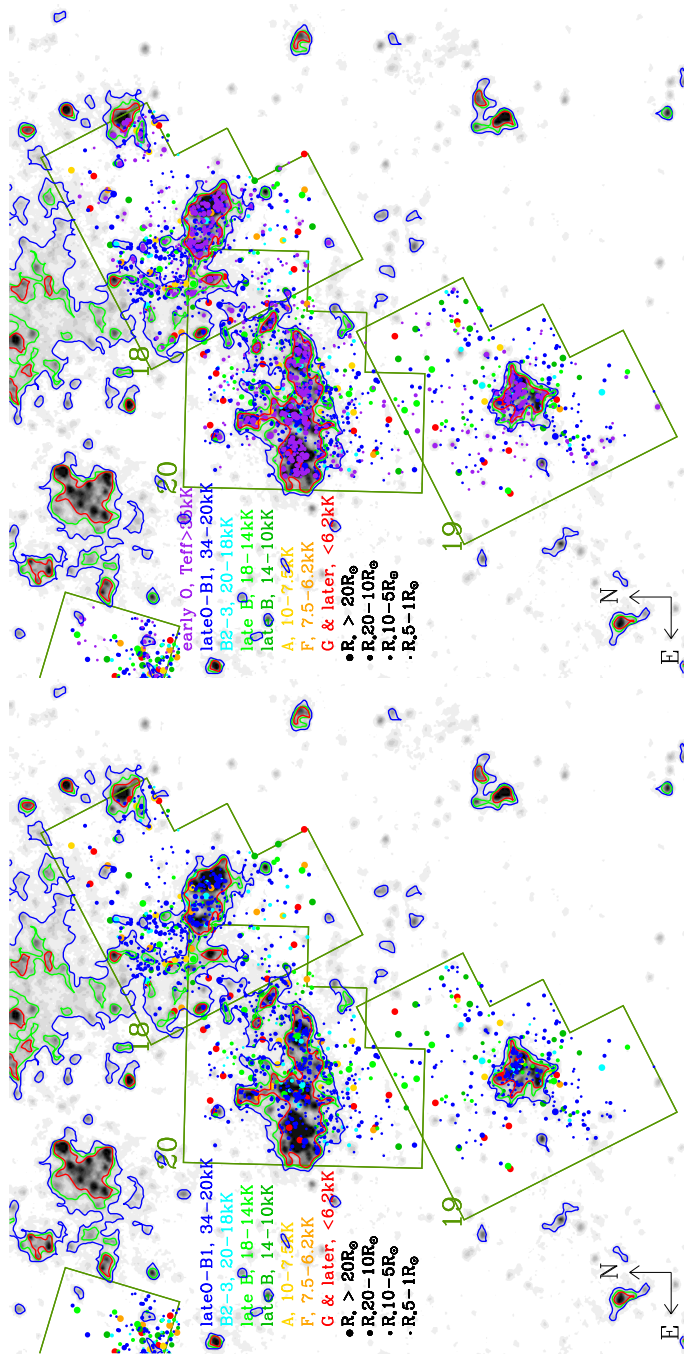


Figure 8: A part of the M33 spiral arm shown in the bottom panels of Figure 7, with stars from Bianchi et al (2013b) color-coded by T_{eff} , overlaid on the GALEX FUV image, and the GALEX-flux defined contours as in Figure 7. In the left panel we omit the hottest stars, to show that these are always found in dense stellar regions where slightly cooler stars also abound. The qualitative picture is informative, although values of T_{eff} from this dataset tend to be systematically overestimated for the hot stars, due to problems in the WFPC2 data (discussed extensively by Bianchi et al. 2012a).

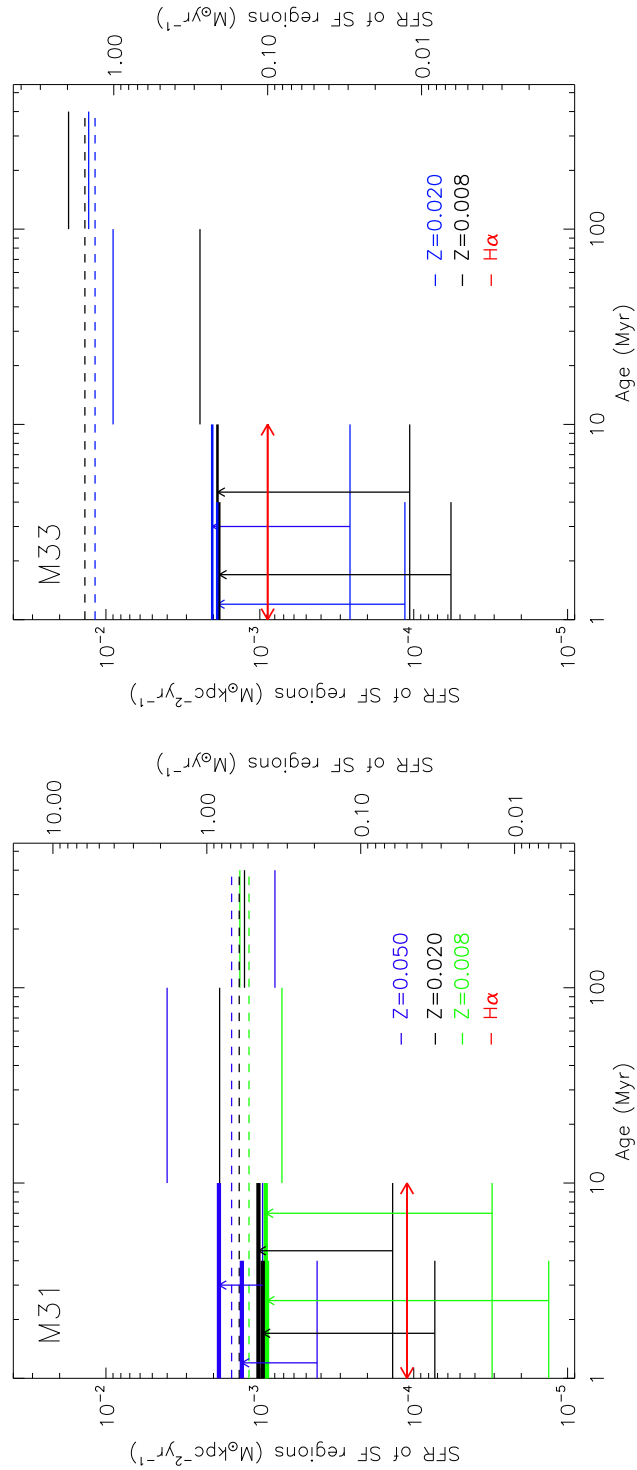


Figure 9: The SFR estimated in recent age intervals from the FUV and NUV integrated fluxes of star-forming regions, for M31 and M33 (figures adapted from the results of Kang et al. 2009, 2013 respectively). The scale on the left Y-axis show SFR per unit area and the right side the SFR. Different colors plot results obtained assuming different metallicity values. Thick lines indicate the SFR estimated from UV and IR data combined (emerged and embedded respectively, see Kang et al. 2009, 2013 for details). Red lines are estimates from $H\alpha$.

**Appendix A. Stellar Model Colors for GALEX FUV and NUV,
several HST filters, and V.**

Table A.1: Stellar model colors (solar metallicity, $\log g=5$ on top and lower gravities following) for E_{B-V} of 0./0.1/0.25/0.5mag (MW extinction with $R_V = 3.1$) in various filters discussed in this paper. The table is available as supplementary material in the online version. Examples are provided here showing the format and content. The first column gives GALEX FUV-NUV, the other columns are 'Filter_i-V', so that more colors can be obtained by combining columns.

Teff (K)	GALEX FUV — GALEX NUV	GALEX NUV — Landolt V	WFC3/UVIS F275W — Landolt V	WFC3/UVIS F336W — Landolt V	ACS WFC F475W ... — ... Landolt V ...
49000.	-1.018 / -1.027 / -1.022 / -0.960	-3.207 / -2.738 / -1.977 / -0.767	-2.750 / -2.451 / -1.959 / -1.150	-2.013 / -1.836 / -1.542 / -1.051	-0.194 / -0.130 / -0.027 / 0.138
48000.	-1.014 / -1.022 / -1.017 / -0.954	-3.198 / -2.729 / -1.969 / -0.759	-2.744 / -2.445 / -1.953 / -1.144	-2.008 / -1.832 / -1.538 / -1.047	-0.193 / -0.129 / -0.027 / 0.139
47000.	-1.008 / -1.016 / -1.011 / -0.948	-3.190 / -2.721 / -1.960 / -0.751	-2.738 / -2.440 / -1.947 / -1.138	-2.004 / -1.827 / -1.534 / -1.043	-0.192 / -0.129 / -0.026 / 0.140
...
30000.	-0.880 / -0.888 / -0.880 / -0.811	-2.856 / -2.387 / -1.627 / -0.421	-2.458 / -2.160 / -1.667 / -0.859	-1.780 / -1.603 / -1.309 / -0.818	-0.151 / -0.089 / 0.014 / 0.178
...
20000.	-0.696 / -0.702 / -0.690 / -0.611	-2.154 / -1.688 / -0.935 / 0.258	-1.881 / -1.584 / -1.097 / -0.294	-1.372 / -1.195 / -0.901 / -0.410	-0.105 / -0.043 / 0.058 / 0.221
...
	...ACS WFC F814W	WFPC2 F170W	WFPC2 F255W	WFPC2 F336W...	
	—	—	—	—	—
	... Landolt V	Landolt V	Landolt V	Landolt V...	

	... WFPC2 F439W	WFPC2 F555W	WFPC2 F814W		
	—	—	—		
	...Landolt V	Landolt V	Landolt V		
		
		